SCIENTIFIC REPORTS

OPEN

Electric-field control of magnetic moment in Pd

Aya Obinata[1], Yuki Hibino[1], Daichi Hayakawa[1], Tomohiro Koyama[1], Kazumoto Miwa[2], Shimpei Ono[2] & Daichi Chiba[1]

Received: 3 March 2014
Accepted: 24 August 2015
Published: 22 September 2015

Several magnetic properties have recently become tunable with an applied electric field. Particularly, electrically controlled magnetic phase transitions and/or magnetic moments have attracted attention because they are the most fundamental parameters in ferromagnetic materials. In this study, we showed that an electric field can be used to control the magnetic moment in films made of Pd, usually a non-magnetic element. Pd ultra-thin films were deposited on ferromagnetic Pt/Co layers. In the Pd layer, a ferromagnetically ordered magnetic moment was induced by the ferromagnetic proximity effect. By applying an electric field to the ferromagnetic surface of this Pd layer, a clear change was observed in the magnetic moment, which was measured directly using a superconducting quantum interference device magnetometer. The results indicate that magnetic moments extrinsically induced in non-magnetic elements by the proximity effect, as well as an intrinsically induced magnetic moments in ferromagnetic elements, as reported previously, are electrically tunable. The results of this study suggest a new avenue for answering the fundamental question of "can an electric field make naturally non-magnetic materials ferromagnetic?"

Application of an electric fields is a useful tool for controlling the magnetism of magnetic materials[1-28] as well as the conductivity of semiconductors. Many studies have been reported, including that of ferromagnetic metals at room temperature[4,7,14,15,17-24,27], using a capacitor structure, with which carrier density can be controlled by applying a gate voltage. Electric-field-induced magnetization switching may drastically reduce power consumption in magnetic recording devices[2,7,8,13,22-25,27].

The changes in material's magnetic properties induced by an electric field are considered to be related to a change in carrier density and, in turn, a shift of the Fermi level. Therefore, we expect that the application of an electric field may make naturally non-magnetic materials ferromagnetic[5,12]. Pt and Pd are usually non-magnetic metals that nearly satisfy the Stoner criterion[29-31]. *Ab initio* calculations have shown that the peak of the density of the states of bulk non-magnetic Pt or Pd is located at an energy near the Fermi level[29], suggesting that an applied electric field may affect the magnetic state in these materials[3,5,12,26]. It is also known that a magnetic moment is induced by the ferromagnetic proximity effect in a Pt or Pd layer deposited on a ferromagnetic metal layer[32-37]. In the present study, we investigated whether the magnetic moment induced in Pd can be electrically controlled. We prepared Pt/Co/Pd structures and observed a clear change in their magnetic moments as a result of applying an electric field to the ferromagnetic surface of the Pd layer. The results indicate that the magnetic moment extrinsically induced in non-magnetic elements by the proximity effect is electrically tunable.

Results

Ferromagnetic proximity effect on Pd deposited on Pt/Co layers. Ta(~3 nm)/Pt(4.1 nm)/Co(t_{Co})/Pd(1.7 nm)/MgO(~2 nm) layers (Pt/Co/Pd samples) from the substrate side were deposited on an intrinsic Si substrate using rf sputtering. Samples without a Pd layer (Pt/Co samples) were also prepared as reference samples to confirm that the magnetic moment was induced in a Pd layer of Pt/Co/Pd samples by the ferromagnetic proximity effect before applying an electric field. Pd and Pt layers were

[1]Department of Applied Physics, Faculty of Engineering, The University of Tokyo, Bunkyo, Tokyo 113-8656, Japan. [2]Central Research Institute of Electric Power Industry, Komae, Tokyo 201-8511, Japan. Correspondence and requests for materials should be addressed to D.C. (email: dchiba@ap.t.u-tokyo.ac.jp)

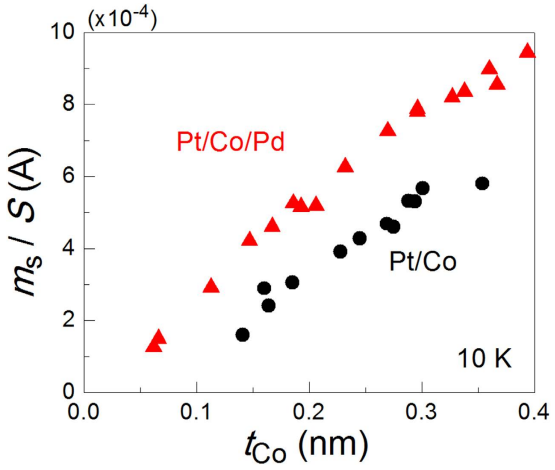

Figure 1. Co thickness t_{Co} dependence of the perpendicular component of the saturation magnetic moment per unit area at 10 K (m_s/S) for Pt/Co (black circles) and Pt/Co/Pd (red triangles) samples. The m_s/S values of the Pt/Co/Pd samples were greater than those of the Pt/Co samples for all t_{Co} values, indicating that a magnetic moment was induced in the Pd layer because of the ferromagnetic proximity effect.

confirmed to have an fcc (111) texture using X-ray diffraction measurement. All of the Pt/Co/Pd and Pt/Co samples we used in this study were confirmed to have perpendicular magnetic anisotropy. Figure 1 shows the t_{Co} dependence of the saturation magnetic moment per unit area (m_s/S) for the both samples. As shown in the figure, the m_s/S values of the Pt/Co/Pd samples were greater than those of the Pt/Co samples for all t_{Co} values, indicating that a magnetic moment was induced in the Pd layer. Assuming that the magnetic moment is uniformly induced in the entire Pd layer, the induced magnetic moment per Pd atom is calculated to be ~$0.1\mu_B$ (μ_B is the Bohr magneton), the order of which is in good agreement with previous studies[32,34,35]. The Pd layer thickness dependence indicates that the magnetic moment induced in the Pd layer saturates at t_{Pd} ~ 2 nm (not shown), suggesting that ~2 nm is the distance limit of the proximity effect from the Co/Pd interface[35]. Thus, in the present sample ($t_{Pd} = 1.7\,nm < 2\,nm$), a finite magnetic moment is expected to be induced in the uppermost Pd atomic layer, but the magnetic moment per Pd atom there is considered to be less than $0.1\mu_B$ because the magnetic moment induced by the ferromagnetic proximity effect is known to decrease with increasing distance from the interface[34,36].

Fabrication of the devices and experimental setup for magnetic moment measurement under applied electric field. An electric-double-layer (EDL) capacitor structure was used to modulate the electron density in the Pd surface[3,4,11,15,16,18,26]. The structure consisted of an Au gate electrode, a polymer film containing an ionic liquid (ionic liquid film)[18], and a Pt/Co/Pd sample (Fig. 2). Two Pt/Co/Pd samples with t_{Co} values of 0.10 and 0.19 nm (samples A and B, respectively) were used in the experiment. The ionic liquid we used was composed of an N,N,N-trimethyl-N-propylammonium ($TMPA^+$) cation and a bis(trifluoromethylsulfonyl)imide ($TFSI^-$) anion. The EDL capacitor was fabricated by simply placing the ionic liquid film with the evaporated Au gate electrode (50 nm) on the Pt/Co/Pd sample. The area covered by the ionic liquid film ($S_{ion\text{-}film}$) was slightly less than the total area of the Pt/Co/Pd sample (S_{total}). Au wires were connected to the Au gate electrode and the Pt/Co/Pd metallic layers to apply a gate voltage V_G between them. A positive V_G corresponded to the direction of increase in the electron density at the Pd surface. The device was introduced into a superconducting quantum interference device magnetometer to measure the magnetic moment directly under the application of V_G[6,18].

Magnetic moment under electric field. Figure 3(a) shows the temperature T dependence of the perpendicular component of the magnetic moment $m_\perp$ divided by S_{total} for both samples A and B under $V_G = +2.0$ and -2.0 V. After V_G was changed at 300 K under a perpendicular magnetic field $\mu_0 H_\perp$ of ~20 mT, T was decreased to 10 K. Subsequently, $\mu_0 H_\perp$ was reduced to nearly zero (1.5 ± 0.1 mT), and the $m_\perp$ shown in Fig. 3(a) was measured by increasing T. Below the Curie temperature T_C, a clear difference in $m_\perp/S_{total}$ was observed with the change in V_G for both samples: a positive (negative) V_G, *i.e.*, larger (smaller) electron density at the Pd surface, resulted in a larger (smaller) $m_\perp/S_{total}$. The difference in $m_\perp$ between $V_G = +2.0$ and -2.0 V ($\Delta m_\perp(\pm 2\,V)$) was found to increase linearly with decreasing temperature, as shown in Fig. 3(b), in which $\Delta m_\perp(\pm 2\,V)$ was divided by $S_{ion\text{-}film}$ because the magnetic moment should be modulated in the area covered by the ionic liquid film. It should be noted that $m_\perp$ was nearly equal to m_s because the squareness ratio $m_\perp/m_s$ of the hysteresis loops was ~1 under $V_G = \pm 2.0$ V at a temperature of at least 10 K, as indicated in the inset of Fig. 3(a). The anomalous Hall effect was used to detect the hysteresis loop under the application of V_G. Although the change in T_C up to 100 K was reported for a Pt/Co sample with a similar device structure[18], T_C was not clearly dependent on V_G in the

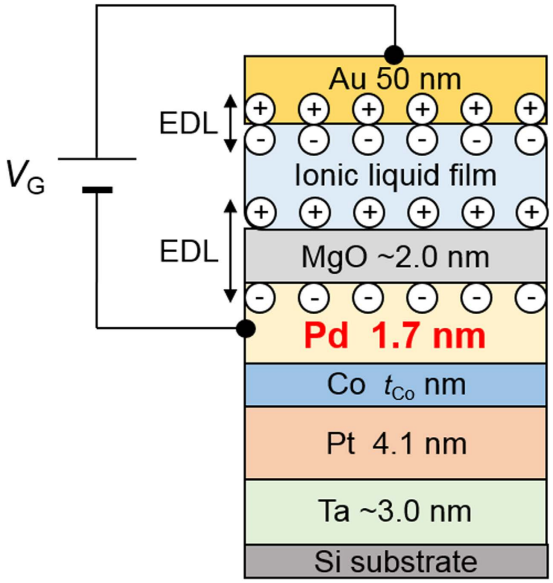

Figure 2. Schematic cross section of the device. A polymer film containing an ionic liquid (ionic liquid film) was used to apply an electric field to the surface of the Pd layer, in which a magnetic moment was induced. By applying a gate voltage V_G, a pair of electric double layers (EDL) was formed at the top and bottom interfaces of the ionic liquid film. The formation of the bottom EDL resulted in a change in the electron density at the surface of the Pd layer. Because of Thomas–Fermi screening, only the electron density at the uppermost Pd layer was expected to be modulated.

present Pt/Co/Pd samples. $\Delta m_\perp(\pm 2\,\mathrm{V})$ deviates significantly from the linear fitting immediately before it intercepts the horizontal axis, as indicated by the downward arrows in Fig. 3(b), which might imply the occurrence of a small change in T_C.

Discussion

We first analysed the temperature dependence of $m_\perp$ for the Pt/Co/Pd and Pt/Co samples. The reduction in the magnetic moment m near T_C can be quantified using a critical exponent β as $m \sim (1 - T/T_C)^\beta$. Figure 4(a) shows a double-logarithmic plot of the normalised $m_\perp$ as a function of $1 - T/T_C$ for several samples with T_C in the range of 157–341 K, including sample B, under an applied electric field (see Table 1 for details of the samples). The value of β was determined from the slope of the linear fitting to the data[37,38] in the range of T_L/T_C (=0.75) to T_H/T_C (=0.87) (see Methods for details of the analysis). The value of $m_\perp$ in the figure was normalised by its value at T_H/T. The value of β was ~0.2 in the Pt/Co samples and ranged from 0.22 to 0.30 in the Pt/Co/Pd samples. From the magnified figure shown in Fig. 4(b), one can clearly see that as $1 - T/T_C$ increased (in other words, as the temperature decreased), the difference in the normalised $m_\perp$ values between the Pt/Co/Pd and Pt/Co samples increased, *i.e.*, the magnetic moment in the Pt/Co/Pd samples increased more rapidly at lower temperatures. This behaviour occurred because the β value of the Pt/Co/Pd samples was higher than that of the Pt/Co samples and/or because the magnetic moment in the ferromagnetic Pd layer is greater at lower temperatures[35,37]. The latter factor is most likely dominant here because the linearity of the normalised $m_\perp$ degrades as $1 - T/T_C$ increases in the double-logarithmic scale. Other important points to consider in understanding the electric-field effect observed in this study are as follows. (i) A larger change in the magnetic moment was observed with the application of V_G in the Pt/Co/Pd samples at lower temperatures, as shown in Figs 3(b) and 4(b). (ii) The data points for the Pt/Co/Pd samples without an applied electric field (indicated by the green symbols in Fig. 4) are almost entirely located between the ones obtained under positive and negative V_G (indicated by the red and blue symbols) at any temperature $T < T_L$. (iii) As shown in Fig. 3(b), the difference between $m_\perp$ under positive and negative V_G ($\Delta m_\perp(\pm 2\,\mathrm{V})$) increased linearly with decreasing temperature. This can probably be attributed to the linear temperature dependence of the magnetic susceptibility of Pd deposited on the layer consisting of the ferromagnetic element[35,37]. These experimental results, which show good reproducibility in similar structures (see Methods), demonstrate that the induced magnetic moment at the surface of the Pd layer was increased and decreased by the application of positive and negative V_G, respectively.

We next analysed the change in $m_\perp$ ($\Delta m_\perp$) for samples A and B upon application of an electric field. Figures 5(a,b) show $\Delta m_\perp/S_{\text{ion-film}}$ at 10 K for both samples as a function of V_G. Each data point was obtained from the temperature dependence of $m_\perp$ at 10 K under each V_G. V_G was applied in the order indicated by the arrows in the figures. Although hysteresis behaviour was observed with round-trip

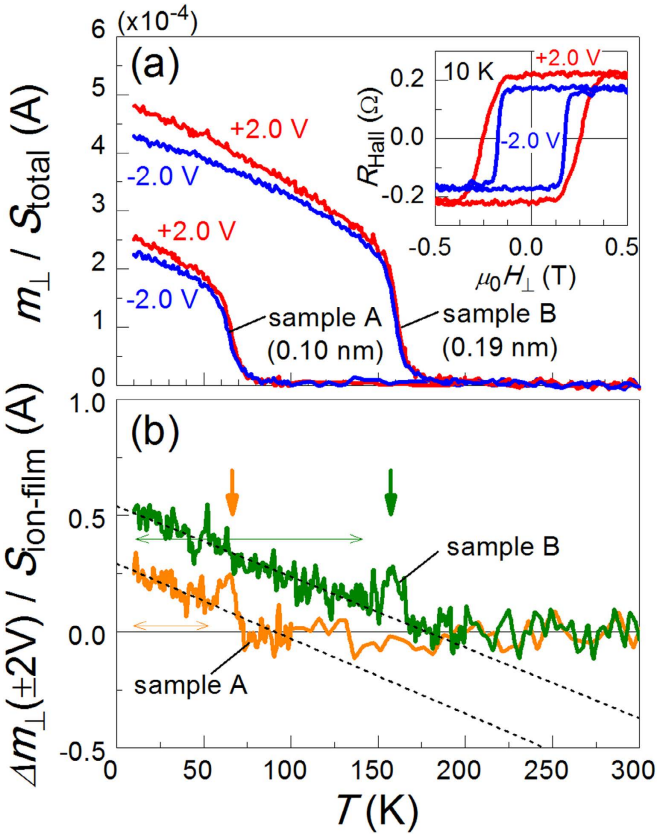

Figure 3. (**a**) Temperature T dependence of the perpendicular component of the magnetic moment $m_\perp$ normalised by the total sample area S_{total} at $V_G = \pm 2.0$ V for samples A (Co layer thickness $t_{Co} = 0.10$ nm) and B ($t_{Co} = 0.19$ nm). Up to 100 K (200 K) for sample A (B), the temperature was increased by 2 K/min, and the averaged $m_\perp$ were measured every 1 K. For averaging, two data points were acquired in the range of 0.2 K, which was much smaller than the temperature interval (1 K) of each averaged $m_\perp$. The inset shows the hysteresis loops observed in the Hall resistance (R_{Hall}) at 10 K at $V_G = \pm 2.0$ V for sample A, from which the squareness ratio of the loops was confirmed to be ~1, regardless of the value of V_G. (**b**) The difference between $m_\perp$ for $V_G = +2.0$ and −2.0 V $\Delta m_\perp(\pm 2\,V)$ is shown as a function of temperature for samples A and B. The $\Delta m_\perp$ (±2 V) shown on the vertical axis was divided by the area covered by the ionic liquid film ($S_{ion\text{-}film}$). The dashed lines indicate the results of the linear fitting using the data within the range indicated by the double-headed horizontal arrows.

V_G application, the tendency of $\Delta m_\perp$ to increase (decrease) with positive (negative) V_G application was reproduced in both samples. The change in the magnetic moment per Pd atom was determined from the linear fitting, as shown in the figures, based on the following assumptions. Pd has an fcc (111) structure, and only the magnetic moment in the uppermost atomic layer was changed because only the electron density there was changed attributed to Thomas–Fermi screening (see Methods for details of the capacitance measurement). The calculated value of the magnetic moment for sample A (B) was $0.050 \pm 0.023\mu_B$ ($0.078 \pm 0.013\mu_B$) per V_G of 1.0 V. The change in the electron number ΔN for sample A (B) per Pd atom and per V_G of 1.0 V was calculated to be 0.049 (0.034). ΔN was determined from the capacitance C of the devices divided by $S_{ion\text{-}film}$.

According to the *ab initio* calculation for Pd, the density-of-states peak appears at an energy level slightly lower than the Fermi level[29]. Thus, a decrease in the electron density should theoretically lead to an increase in the magnetic moment[5,12]. Our results, however, were the opposite. Support from theoretical calculations is clearly needed to understand our results. The state of the Pd in our sample structure was different from that in the bulk case in the following respects: (1) the magnetic moment was already induced in the Pd layer (thus, spin splitting was already induced); and (2) the Pd layer was very thin, and interfaces were formed between the Co and MgO layers. In addition, we note that in a Pt/Co system, in which the electric field induced changes in T_C and a magnetic moment was reported[17,18], *ab initio* calculations indicated that the number of 3*d* electrons can be decreased even when an electric field is applied in the direction of increase in the total electron number because the number of *sp* electrons increases[28]. This explains the discrepancy between the experimental results and the outcome suggested by the Slater–Pauling curve for the Co case. This scenario may be applicable even to the present 4*d* electron system

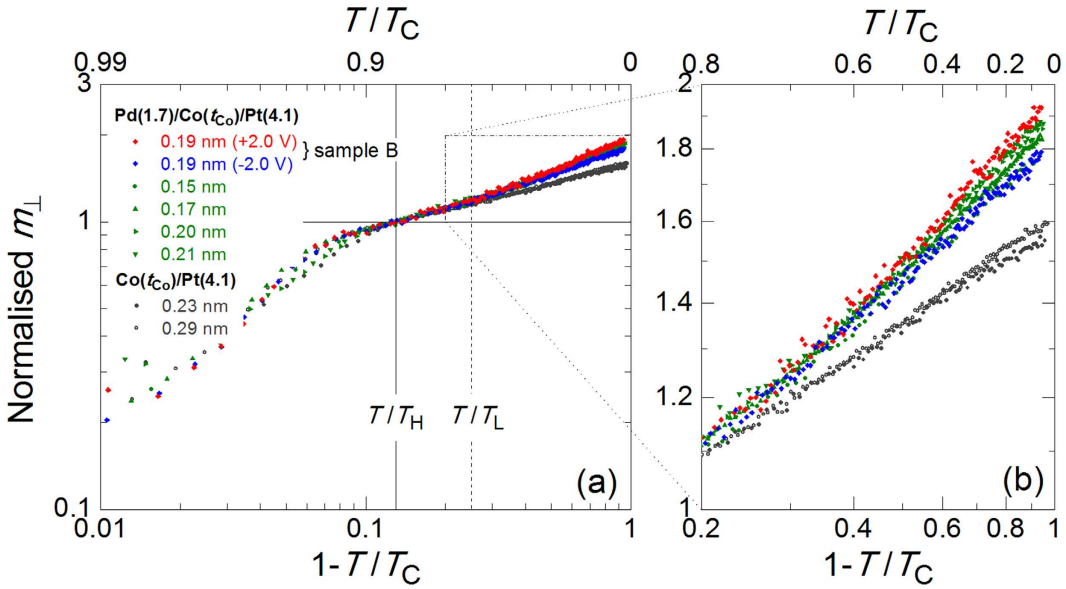

Figure 4. (**a**) Double-logarithmic plot of the normalised $m_\perp$ as a function of $1 - T/T_C$ for several samples listed in Table 1. (**b**) Magnified view of the region indicated by the dashed-dotted line in (**a**). T/T_H and T/T_L in the figure indicates the range for the fitting performed to obtain the critical exponent β. The values of $m_\perp$ on the vertical axis were normalised by the value at T/T_H. The magnetic moment in the Pt/Co/Pd samples increased more rapidly than that in the Pt/Co samples as $1 - T/T_C$ increased (in other words, as the temperature was reduced). The data points for the Pt/Co/Pd samples to which an electric field were not applied (green symbols) were confirmed to lie almost entirely between the ones obtained under the application of positive and negative V_G to sample B (red and blue symbols) at a temperature $T < T_L$.

	V_G (V)	t_{Pd} (nm)	t_{Co} (nm)	t_{Pt} (nm)	T_C (K)	β
sample B	+2.0	1.7	0.19	4.1	167	0.27
	-2.0	1.7	0.19	4.1	166	0.25
Pt/Co/Pd	-	1.7	0.15	4.1	157	0.22
	-	1.7	0.17	4.1	178	0.26
	-	1.7	0.21	4.1	195	0.30
Pt/Co	-	-	0.23	4.1	228	0.21
	-	-	0.29	4.1	341	0.20

Table 1. Properties of the Pt/Co/Pd and Pt/Co samples used in Fig. 4. The thicknesses of the Pd, Co, and Pt layers (t_{Pd}, t_{Co}, and t_{Pt}); T_C; and the critical exponent β determined from the fitting (see Methods for details of the determination) are summarised.

(Pd). Furthermore, reversible chemical effects, such as the migration of oxygen atoms from the MgO[27] cap or of hydrogen absorption in the Pd layer[39] by V_G applications might be related to a change in the electron state and thus to a change in the magnetic moment induced in Pd. From an experimental perspective, the next challenge is to induce ferromagnetism electrically in naturally non-magnetic materials beyond that attributable to the ferromagnetic proximity effect.

Methods

Determination of T_C. Figures 6(a,b) show the Arrott plots[40] for two reference samples, a Pt/Co/Pd sample with $t_{Co} = 0.20$ nm and $t_{Pd} = 1.7$ nm and a Pt/Co sample with $t_{Co} = 0.32$ nm, respectively. From the

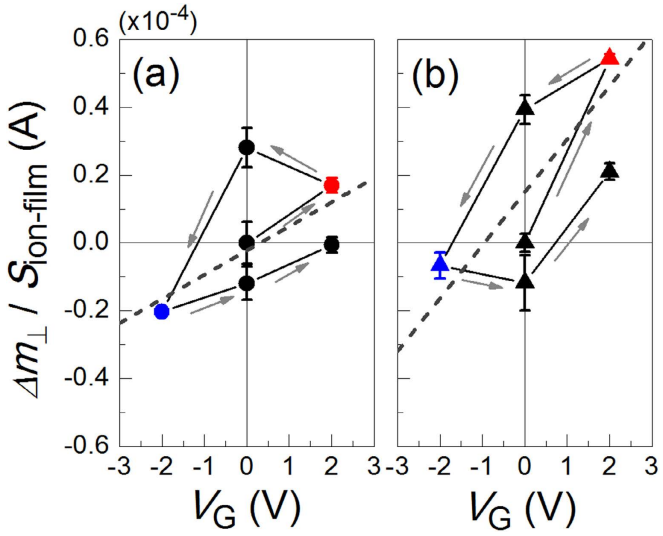

Figure 5. Change in the perpendicular component of the magnetic moment ($\Delta m_\perp$) at 10 K normalised by $S_{\text{ion-film}}$ for samples (a) A and (b) B as a function of V_G. V_G was changed at 300 K, and the temperature was reduced to measure each value of $m_\perp$ at 10 K. The dashed line indicates the linear fitting to the averaged $\Delta m_\perp/S$ at each V_G, from which the change in the magnetic moment per Pd atom was determined.

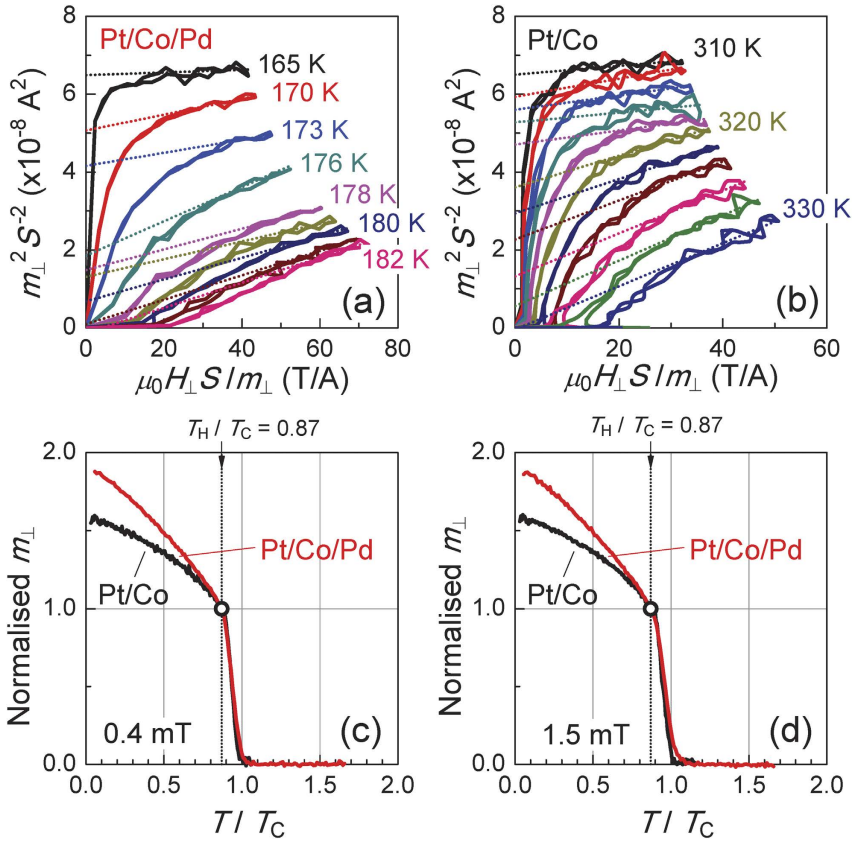

Figure 6. (**a**,**b**) The Arrott plots for the Pt/Co/Pd and the Pt/Co reference samples, respectively. (**c**,**d**) The normalised temperature (T/T_C) dependence of the normalised magnetic moment ($m_\perp$) for both reference samples at 0.4 (±0.1) mT and 1.5 (±0.1) mT, respectively. The vertical axes in (**c**,**d**) were normalised by the $m_\perp$ value at T/T_C=0.87.

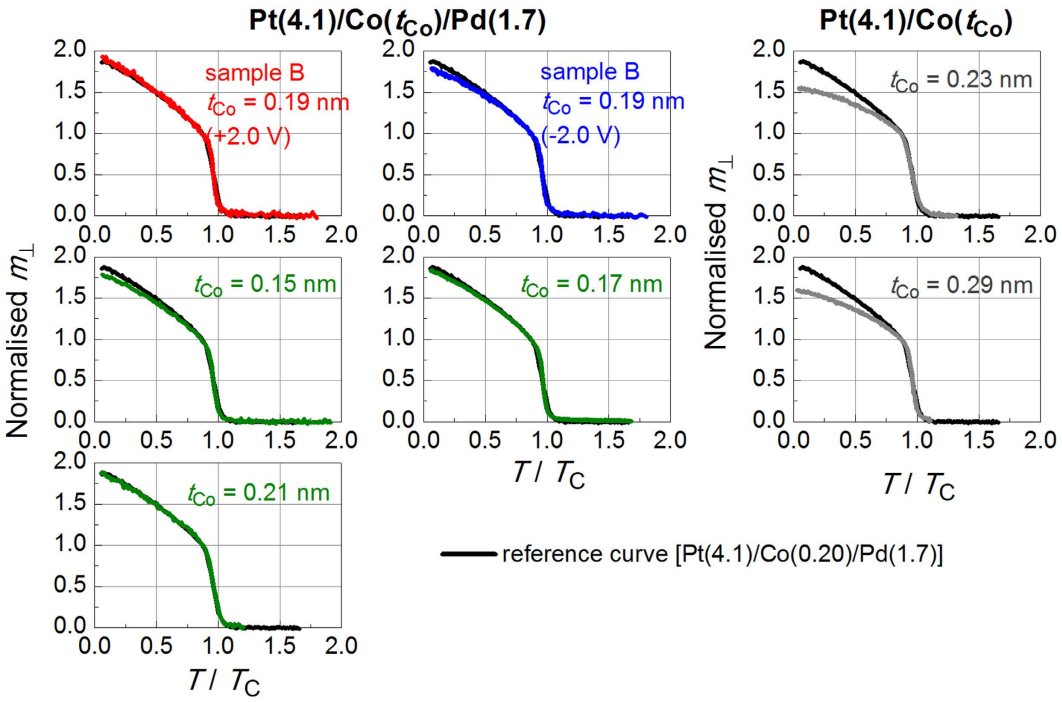

Figure 7. T/T_C dependence of the normalised $m_\perp$ for all samples listed in Table 1. The black line indicates the results obtained for the Pt/Co/Pd reference sample. The results are indicated by coloured lines. All $m_\perp$ was measured at 1.5 (±0.1) mT and the vertical axes were normalised by the $m_\perp$ value at $T/T_C = 0.87$.

plots, the T_C of the Pt/Co/Pd (the Pt/Co) reference sample was determined to be 181 (329) K. The T/T_C dependence of $m_\perp$ at $\mu_0 H_\perp = 0.4$ (±0.1) mT for both reference samples is shown in Fig. 6(c), in which the vertical axis is normalised by an $m_\perp$ value at $T/T_C = 0.87$. In both samples, $m_\perp$ decreased rapidly below T_C. This was most likely because of the formation of a multi-domain state, as observed in similar Pt/Co samples[17,41]. The important point is that, as long as $\mu_0 H_\perp$ was the same (see Figs 6(c,d)), the two curves for Pt/Co/Pd and Pt/Co reference samples overlap very well in this temperature region, even though these samples have different sample structures and T_C values. This suggests that as long as T_C is known for one reference sample, one can determine the T_C of another sample by comparing the $m_\perp$–T curves. Figure 7 presents a summary of the comparison of the results for the samples listed in Table 1 (coloured line) and the Pt/Co/Pd reference sample (black line). Adjusting the T_C values of the samples resulted in the normalised curves overlapping well with the reference curve. The T_C values of the samples listed in Table 1 were determined in this way. The difference in T_C for these samples determined using the Pt/Co/Pd and Pt/Co reference samples was at most 1–2%. The Arrott–Noakes (AN) plot[42] may provide more accurate T_C for the present two-dimensional system. However, the difference in T_C determined from the Arrott and AN plots is only 1–2%[17]. In comparing many samples without difficulty and confirming the most important finding of this study, *i.e.*, the induced magnetic moment in the Pd layer being increased or decreased by applying an electric field, we believe that the Arrott plot and the above-mentioned way of determining T_C were useful method. We note that using a similar Pt/Co/Pd sample with a T_C of ~190 K (not shown in Table 1) confirms the reproducibility of the results, *i.e.*, the data points for the sample without an applied electric field are almost entirely located between the points obtained for similar samples under positive and negative V_G at any temperature $T < T_L$.

Determination of the critical exponent β. The value of β was determined from the slope of the linear line fitted to the normalised $m_\perp$ data in the range between T_L/T_C (=0.75) and T_H/T_C (=0.87) on a double-logarithmic scale (see Fig. 4a). The fitting range was determined from the linearity of the data. It was difficult to perform a reliable fitting to the data for sample A because there were not enough data points in the fitting range.

Capacitance measurement. The capacitance C of samples A and B was measured using a capacitance meter and applying an ac voltage with an amplitude of 0.1 V and frequency f of 100 Hz. In addition, the f dependence of C for a similar device showed that C increases slightly with decreasing f. Although further experiments are needed to determine an accurate value for ΔN under a dc gate voltage, the value of C estimated using the above experimental results for $f = 0.01$ Hz, which was the lowest value of f in the

experiment, was used to calculate the ΔN described in this report. The values of $C/S_{\text{ion-film}}$ at $f = 0.01$ Hz for samples A and B were 12 and 8.3 μF/cm^2, respectively.

References

1. Ohno, H. *et al.* Electric-field control of ferromagnetism. *Nature* **408,** 944–946 (2000).
2. Chiba, D., Yamanouchi, M., Matsukura, F. & Ohno, H. Electrical manipulation of magnetization reversal in a ferromagnetic semiconductor. *Science* **301,** 943–945 (2003).
3. Drings, H. *et al.* Tuneable magnetic susceptibility of nanocrystalline palladium. *Appl. Phys. Lett.* **88,** 253103 (2006).
4. Weisheit, M. *et al.* Electric field-induced modification of magnetism in thin-film ferromagnets. *Science* **315,** 349–351 (2007).
5. Kudasov, Y. B. & Korshunov, A. S. Surface ferromagnetism of palladium induced by strong electric field. *Phys. Lett. A* **364,** 348–351 (2007).
6. Sawicki, M. *et al.* Experimental probing of the interplay between ferromagnetism and localization in (Ga, Mn)As. *Nature Phys.* **6,** 22–25 (2010).
7. Maruyama, T. *et al.* Large voltage-induced magnetic anisotropy change in a few atomic layers of iron. *Nature Nanotech.* **4,** 158–161 (2009).
8. Stöhr, J., Siegmann, H. C., Kashuba, A. & Gamble, S. J. Magnetization switching without charge or spin currents. *Appl. Phys. Lett.* **94,** 072504 (2009).
9. Nakamura, K. *et al.* Giant modification of the magnetocrystalline anisotropy in transition-metal monolayers by an external electric field. *Phys. Rev. Lett.* **102,** 187201 (2009).
10. Tsujikawa, M. & Oda, T. Finite electric field effects in the large perpendicular magnetic anisotropy surface Pt/Fe/Pt(001): A first-principles study. *Phys. Rev. Lett.* **102,** 247203 (2009).
11. Endo, M. *et al.* Electric double layer transistor with a (Ga, Mn)As channel. *Appl. Phys. Lett.* **96,** 022515 (2010).
12. Sun, Y., Burton, J. D. & Tsymbal, E. Y. Electrically driven magnetism on a Pd thin film. *Phys. Rev. B* **81,** 064413 (2010).
13. Chiba, D., Nakatani, Y., Matsukura, F. & Ohno, H. Simulation of magnetization switching by electric-field manipulation of magnetic anisotropy. *Appl. Phys. Lett.* **96,** 192506 (2010).
14. Endo, M., Kanai, S., Ikeda, S., Matsukura, F. & Ohno, H. Electric-field effects on thickness dependent magnetic anisotropy of sputtered MgO/$Co_{40}Fe_{40}B_{20}$/Ta structures. *Appl. Phys. Lett.* **96,** 212503 (2010).
15. Zhernenkov, M. *et al.* Electric-field modification of magnetism in a thin CoPd film. *Phys. Rev. B* **82,** 024420 (2010).
16. Yamada, Y. *et al.* Electrically induced ferromagnetism at room temperature in cobalt-doped titanium dioxide. *Science* **332,** 1065–1067 (2011).
17. Chiba, D. *et al.* Electrical control of the ferromagnetic phase transition in cobalt at room temperature. *Nature Mater.* **10,** 853–856 (2011).
18. Shimamura, K. *et al.* Electrical control of Curie temperature in cobalt using an ionic liquid film. *Appl. Phys. Lett.* **100,** 122402 (2012).
19. Bauer, U., Emori, S. & Beach, G. S. D. Electric field control of domain wall propagation in Pt/Co/GdOx films. *Appl. Phys. Lett.* **100,** 192408 (2012).
20. Schellekens, A. J., van den Brink, A., Franken, J. H., Swagten, H. J. M. & Koopmans, B. Electric-field control of domain wall motion in perpendicularly magnetized materials. *Nature Comm.* **3,** 847 (2012).
21. Chiba, D. *et al.* Electric-field control of magnetic domain-wall velocity in ultrathin cobalt with perpendicular magnetization. *Nature Comm.* **3,** 888 (2012).
22. Shiota, Y. *et al.* Induction of coherent magnetization switching in a few atomic layers of FeCo using voltage pulses. *Nature Mater.* **11,** 39–43 (2012).
23. Wang, W.-G., Li, M., Hageman, S. & Chien, C. L. Electric-field-assisted switching in magnetic tunnel junctions. *Nature Mater.* **11,** 64–68 (2012).
24. Kanai, S. *et al.* Electric field-induced magnetization reversal in a perpendicular-anisotropy CoFeB-MgO magnetic tunnel junction. *Appl. Phys. Lett.* **101,** 122403 (2012).
25. Chiba, D., Ono, T., Matsukura, F. & Ohno, H. Electric field control of thermal stability and magnetization switching in (Ga, Mn) As. *Appl. Phys. Lett.* **103,** 142418 (2013).
26. Shimizu, S. *et al.* Electrically tunable anomalous Hall effect in Pt thin films. *Phys. Rev. Lett.* **111,** 216803 (2013).
27. Bauer, U. *et al.* Magneto-ionic control of interfacial magnetism. *Nature Mater.* **14,** 174–181 (2015).
28. Oba, M. *et al.* Electric-field-induced modification of the magnon energy, exchange interaction, and Curie temperature of transition-metal thin films. *Phys. Rev. Lett.* **114,** 107202 (2015).
29. MacDonald, A. H., Daams, J. M., Vosko, S. H. & Koelling, D. D. Influence of relativistic contributions to the effective potential on the electronic structure of Pd and Pt. *Phys. Rev. B* **23,** 6377–6398 (1981).
30. Sigalas, M. M. & Papaconstantopoulos, D. A. Calculations of the total energy, electron-phonon interaction, and Stoner parameter for metals. *Phys. Rev. B* **50,** 7255–7261 (1994).
31. Shinohara, T., Sato, T. & Taniyama, T. Surface ferromagnetism of Pd fine particles. *Phys. Rev. Lett.* **91,** 197201 (2003).
32. Gradmann, U. & Bergholz, R. Magnetization of Pd (111) films by contact with ferromagnetic Ni (111) films. *Phys. Rev. Lett.* **52,** 771–774 (1984).
33. den Broeder, F. J. A., Donkersloot, H. C., Draaisma, H. J. G. & de Jonge, W. J. M. Magnetic properties and structure of Pd/Co and Pd/Fe multilayers. *J. Appl. Phys.* **61,** 4317–4319 (1987).
34. Wu, R., Li, C. & Freeman, A. J. Structual, electronic and magnetic properties of Co/Pd(111) and Co/Pt(111). *J. Magn. Magn. Mater.* **99,** 71–80 (1991).
35. Cheng, L. *et al.* Pd polarization and interfacial moments in Pd-Fe multilayers. *Phys. Rev. B* **69,** 144403 (2004).
36. Suzuki, M. *et al.* Depth profile of spin and orbital magnetic moments in a subnanometer Pt film on Co. *Phys. Rev. B* **72,** 054430 (2005).
37. Hase, T. P. A. *et al.* Proximity effects on dimensionality and magnetic ordering in Pd/Fe/Pd trialyers. *Phys. Rev. B* **90,** 104403 (2014).
38. Dürr, W. *et al.* Magnetic phase transition in two-dimensional ultrathin Fe films on Au(100). *Phys. Rev. Lett.* **62,** 206–209 (1989).
39. Manago, T., Otani, Y., Miyajima, H. & Akiba, E. Magnetic properties and Pd-H miscibility gap in Ni/Pd composite fine particles. *J. Appl. Phys.* **79,** 5126–5128 (1996).
40. Arrott, A. Criterion for ferromagnetism from observations of magnetic isotherms. *Phys. Rev.* **108,** 1394–1396 (1957).
41. Koyama, T. *et al.* Dependence of Curie temperature on Pt layer thickness in Co/Pt system. *Appl. Phys. Lett.* **106,** 132409 (2015).
42. Arrott, A. & Noakes, J. E. Approximate equation of state for nickel near its critical temperature. *Phys. Rev. Lett.* **19,** 786–789 (1967).

Acknowledgements
The authors thank Prof. Kozuka, Prof. Kawasaki, and Prof. Tsukazaki for their technical assistance. This work was partly supported by a Grant-in-Aid for Scientific Research (S) (No. 25220604) and (B) (No. 26288115) from JSPS and a research grant from the Foundation for the Promotion of Ion Engineering. A portion of this work was performed using the facilities of the Cryogenic Research Center of the University of Tokyo.

Author Contributions
D.C. planned and supervised the study. A.O., Y.H. and D.H. prepared samples. A.O. and D.H. fabricated the device. K.M. and S.O. provided the ionic liquid films. A.O., T.K. and D.C. set up the measurement apparatus. A.O. collected and analysed the data. Y.H. collected the data on the dependence of the magnetic moment on the Pd layer thickness. D.H. checked the reproducibility of the electric-field effect. A.O., T.K. and D.C. wrote the manuscript. All authors discussed the results.

Additional Information
Competing financial interests: The authors declare no competing financial interests.

How to cite this article: Obinata, A. *et al.* Electric-field control of magnetic moment in Pd. *Sci. Rep.* **5**, 14303; doi: 10.1038/srep14303 (2015).